Online Resource 1

Linear Regressions of Estimates of ^{18}F-FDG Parameters from both Models

Slopes and intercepts of linear regressions between parameter estimates of the delayed input function model and the right heart input function model are given in Table S1.

Table S1. Slopes and intercepts for linear regressions of delayed input function and right heart input function model parameter estimates.

	Control					
	slope (m)			intercept (y_{int})		
	estimate	SE	p (m=1)	estimate	SE	p (y_{int}=0)
k_1	0.579	0.086	<0.001	0.011	0.011	0.338
k_2	0.554	0.158	0.012	0.136	0.114	0.248
k_3	1.128	0.052	0.025	-0.001	0.001	0.299
F_B	1.272	0.040	<0.001	0.005	0.004	0.187
F_e	0.865	0.048	0.012	0.004	0.008	0.614
K_i	0.967	0.010	0.005	0.000	0.000	0.200
	LPS					
	slope (m)			intercept (y_{int})		
	estimate	SE	p (m=1)	estimate	SE	p (y_{int}=0)
k_1	0.701	0.096	0.007	-0.007	0.007	0.921
k_2	0.771	0.093	0.026	-0.036	0.045	0.435
k_3	1.006	0.051	0.908	-0.001	0.002	0.620
F_B	1.076	0.030	0.022	0.014	0.003	<0.001
F_e	1.042	0.021	0.063	-0.009	0.004	0.047
K_i	0.969	0.200	0.139	0.000	0.000	0.285
	Lavage + LPS					
	slope (m)			intercept (y_{int})		
	estimate	SE	p (m=1)	estimate	SE	p (y_{int}=0)
k_1	1.013	0.061	0.838	-0.012	0.004	0.014
k_2	0.475	0.064	<0.001	0.061	0.017	0.003
k_3	0.910	0.057	0.131	0.001	0.002	0.551
F_B	1.036	0.027	0.200	0.014	0.003	<0.001
F_e	1.024	0.013	0.086	-0.001	0.005	0.851
K_i	0.966	0.013	0.020	0.000	0.000	0.486

SE, standard error of the estimate; m, slope; y_{int}, y-intercept. For each ^{18}F-FDG parameter, the linear regression of the delayed input function model parameters onto the right heart input function model parameters was computed. To compare regressions with the line of identity, p values are given for the null hypotheses that the regression slope was equal to 1 and the regression intercept was equal to 0.

Online Resource 2

Bland-Altman Analysis and ROI Dependence of Agreement between Perfusion Estimates

In this supplement, we present additional analysis of agreement between measurements of mean-normalized perfusion derived using the ^{18}F-FDG and ^{13}NN imaging techniques. Figure S1 shows Bland-Altman style plots comparing the two measurement techniques. Figure S2 shows the dependence of the level of agreement on ROI size in each condition. Agreement between the techniques decreased with smaller ROI sizes, with acceptable levels of agreement maintained down to ROI volumes of about 50 mL.

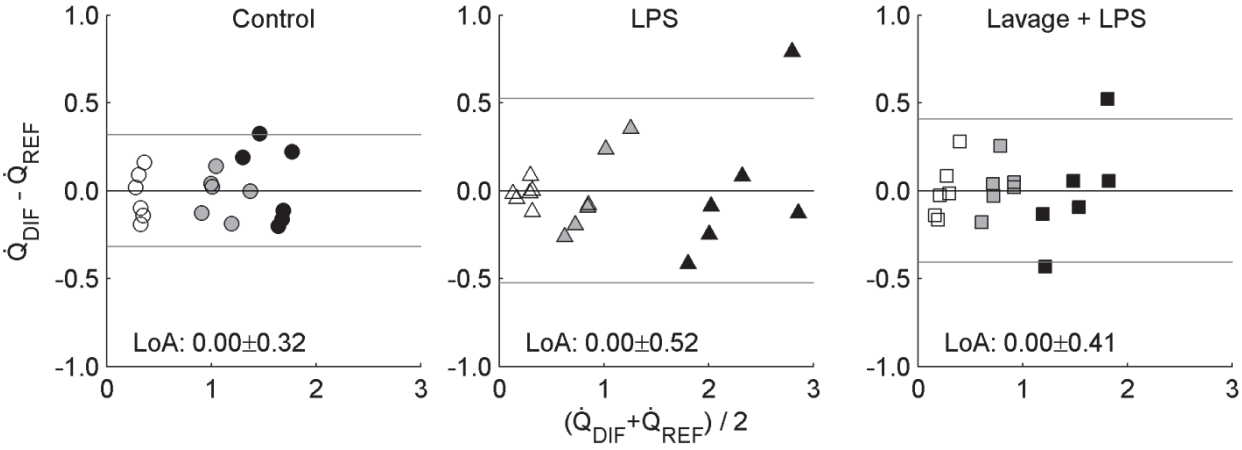

Figure S1. Bland-Altman plots of differences between perfusion measured with the delayed input function model (Q_{DIF}) and perfusion measured with the reference ^{13}NN method (Q_{REF}) in three isogravitational ROIs in each condition (black=dependent, gray=middle, white=non-dependent region). Because both sets of measurements were mean-normalized, the average difference (i.e., the bias) was necessarily zero. Differences were not correlated with perfusion magnitude in any of the conditions. Gray lines indicate limits of agreement (LoA), defined as 95% confidence intervals around the average difference of 0. ROI volumes averaged 183±60 mL (Control), 150±44 mL (LPS), 95±37 mL (Lavage + LPS).

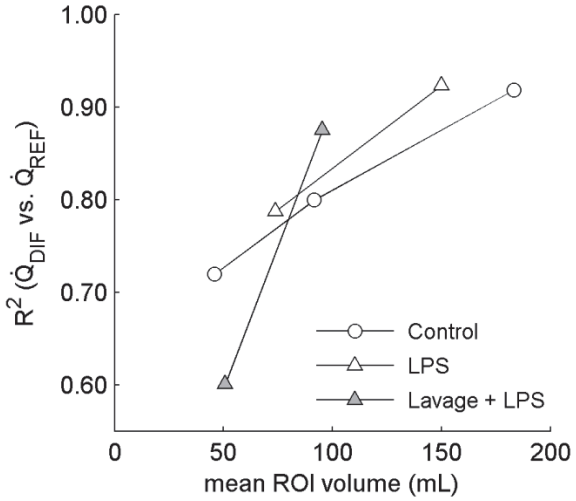

Figure S2. Agreement between Q_{DIF} and Q_{REF} versus ROI size. Agreement was defined as the coefficient of determination (R^2) for the linear regression of Q_{DIF} onto Q_{REF}. In the Control group, ROI configurations of 3, 6, and 12 vertically divided ROIs were studied. In the Lung Injury group, each lung (right = LPS, left = Lavage + LPS) was divided into either 3 or 6 ROIs. The agreement between the techniques decreased with smaller ROI sizes, but acceptable agreement was observed down to ROI volumes of about 50 mL.

Online Resource 3

Effect of Cardiac Output on Regional Delay Measurements

In order to estimate and subtract out the pulmonary artery delay, our technique relies on measurements of cardiac output, which are not always available in clinical settings. However, cardiac output can often be estimated with reasonable accuracy using other physiological measurements and patient characteristics. Therefore, we examined how errors in cardiac output would influence our measurements of the regional lung input function delay (t_{lung}). Based on Equation 1 of the main text, we estimated the pulmonary artery delay (t_{PA}) as:

$$t_{PA} = \frac{V_{PA}}{CO} \quad \text{(S1)}$$

where V_{PA} is the pulmonary artery blood volume and CO is the cardiac output (i.e., pulmonary artery blood flow). As derived in the main text, t_{PA} is subtracted from the total regional delay measured from ^{18}F-FDG kinetics (t_{delay}) to compute the regional lung-specific delay (t_{lung}). Thus, t_{lung} has a non-linear dependence on cardiac output given by:

$$t_{lung} = t_{delay} - \frac{V_{PA}}{CO} \quad \text{(S2)}$$

Therefore, the influence of errors in CO on measurements of t_{lung} would depend on the specific values of t_{delay} and V_{PA}. When t_{delay} is relatively large compared to t_{PA}, errors in t_{lung} caused by over or underestimation of CO would be relatively small. Our experimental measurements of t_{PA} and t_{delay} suggest that this was indeed the case. In the control group, the t_{PA} / t_{delay} fraction averaged 0.18±0.09 (mean±SD), and in the lung injury group 0.17±0.08.

We also performed simple simulations to determine the effect of errors in CO on t_{lung}. For all studied ROIs, we introduced errors in CO ranging from -30% to 30% and calculated the resulting errors in t_{lung}, using experimental values of t_{delay} and V_{PA} for each ROI. Consistent with

Equation S2, errors in t_{lung} showed a non-linear dependence on errors in CO, with underestimation of CO leading to larger error magnitude than overestimation (Figure S3). However, errors in t_{lung} were notably smaller than those in CO, with average error in t_{lung} remaining under 10% even for 30% error in CO (Figure S3). Thus, the accuracy of the parameter t_{lung} is not critically dependent on the accuracy of cardiac output estimates, allowing for application of the technique in settings where cardiac output cannot be measured and must be estimated from surrogate parameters.

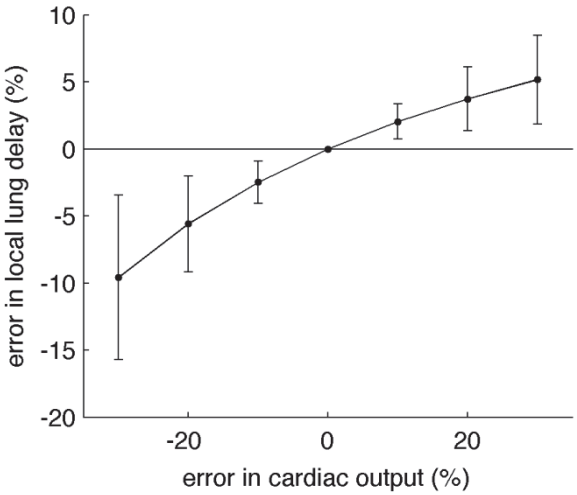

Figure S3. Dependence of error in local lung delay (t_{lung}) on error in cardiac output for data from all animals and regions-of-interest. Mean±SD are shown for each point.